ELSEVIER

S0032-3861(96)00622-2

Polymer Vol. 37 No. 22, pp. 4937–4944, 1996

0032-3861/96/$15.00+0.00

Helical twisting power of chiral side-chain liquid crystal copolymers

J. M. G. Cowie* and T. Hinchcliffe
Department of Chemistry, Heriot-Watt University, Edinburgh EH14 4AS, UK
(Received 23 October 1995; revised 24 April 1996)

A series of copolymers, comprising a chiral mesogen ((*S*)-(−)-4-methoxyphenyl-4′-(2-acryloyloxy)propoxy benzoate) and a non-chiral mesogenic comonomer (4-cyanophenyl-4′-(6-acryloyloxy) benzoate), was prepared, and each sample characterized physically and optically. The copolymers were found to exhibit a chiral nematic phase when the mole fraction of the chiral monomer in the copolymer was greater than 0.2. Films of these samples selectively reflect light of wavelength λ_R, which is inversely proportional to the mole fraction of chiral monomer in the copolymer. The values of λ_R were determined at a fixed reduced temperature T^* by differential absorption spectrometry and by specular reflectivity measurements. Plots of $(1/\lambda_R)$ against mole fraction of the chiral mesogen in the copolymer gave values of the helical twisting power of 5×10^{-3} mm^{-1}, which is lower than observed for cholesterol-containing polymers but comparable to or greater than values reported for side-chain liquid crystal polymers with alternative chiral centres.

(Keywords: copolymers; liquid crystal; chiral nematic; selective reflection)

INTRODUCTION

Thermotropic side-chain liquid crystal polymers (SCLCPs) that have a chiral centre placed in the vicinity of the mesogenic unit can enter into liquid crystal phases, some of which possess interesting optical properties. When the phase formed is the chiral nematic (N*) one, the directors in succeeding layers of the anisotropic liquid are displaced on average by a few degrees from their neighbours. This regular twisting occurs about an axis perpendicular to the director and generates a helical structure with a defined pitch *P*. Each helical stack then possesses periodicity along its *z* axis, and in well-aligned samples with this axis normal to the supporting substrate this acts as a diffraction lattice capable of reflecting 50% of the initial intensity of light (i.e. of one circular polarization) of a peak wavelength λ_R[1]. This is related to the pitch length by a simple equation[2]:

$$\lambda_R = \tilde{n}P \quad (1)$$

where $\tilde{n}$ is the mean refractive index of the material and for normally incident light. As the dimensions of these helical structures tend to be of the same order of magnitude as the wavelengths of visible light, the thin layers often appear coloured, depending on the value of *P*. The pitch of the helical structure is sensitive to changes in temperature, polymer structure and the compositional changes brought about by copolymerization of the chiral monomer with non-chiral mesogenic or non-mesogenic monomers[1,3,4]. While copolymerization can alter the temperature range over which the N* phase exists and also the pitch *P*[5–7], the positions of the chiral centres with respect to the mesogenic unit can change the helical twisting power. These effects will be examined in this and subsequent papers.

When synthesizing chiral mesogenic monomers to use in the preparation of comb-branch polymers, one has the choice of incorporating the chiral centre in the tail unit of the mesogen or alternatively, as was first reported from this laboratory[5], in the spacer unit between the mesogen and the polymer backbone.

The latter approach allows greater latitude for subsequent modification of the terminal unit, and this strategy was adopted to prepare (*S*)-(−)-4-methoxyphenyl-4′-(2-acryloyloxy)propoxy benzoate (**1**). Property modification was achieved by copolymerizing **1** with a non-chiral mesogenic monomer 4-cyanophenyl-4′-(6-acryloyloxy) benzoate (**2**). The effect of copolymer composition on the selective reflection of visible light is examined here.

EXPERIMENTAL

Materials

Monomers were synthesized using multistep procedures.

(S)-(−)-4-Methoxyphenyl-4′-(2-acryloyloxy)propoxy benzoate (1). The initial chiral building block 2-(tetrahydro-2-pyranyloxy)-1-propyl *p*-toluene sulfonate (TPT) was prepared from (*S*)-(−)-ethyl lactate, as described previously[5]. The target monomer (**1**) was synthesized in three further steps, as shown in *Scheme 1*.

Compound 3. Sodium hydride (2.05 g, 85 mmol) was slurried in dimethyl formamide (DMF) (15 ml) under a flow of nitrogen and a solution of 4-methoxyphenyl-4′-hydroxybenzoate (20.6 g, 84 mmol) in DMF (90 ml) was added dropwise to the stirred slurry. Stirring was

* To whom correspondence should be addressed

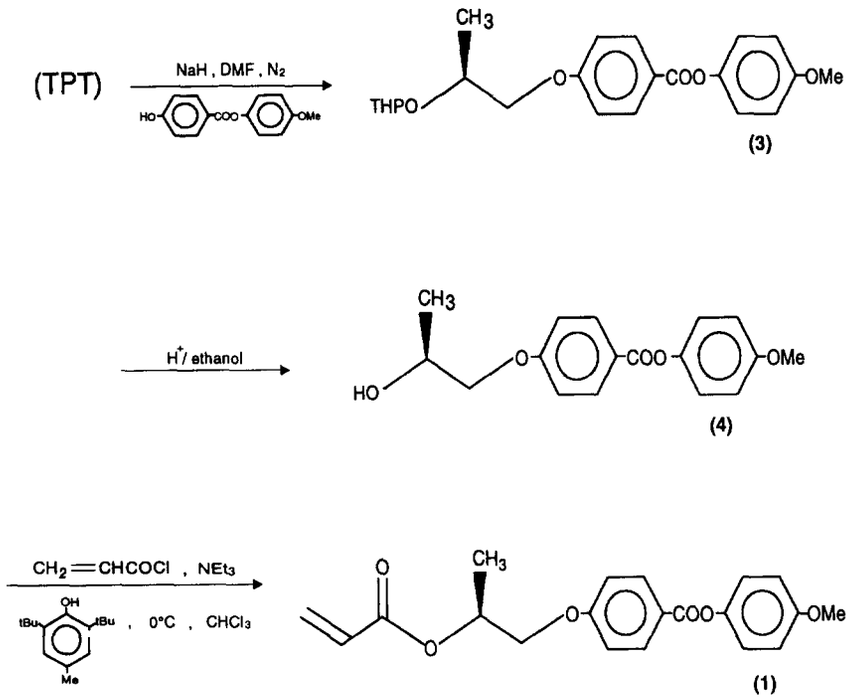

Scheme 1

Table 1 ^{13}C n.m.r. peak chemical shift values for compound **4**

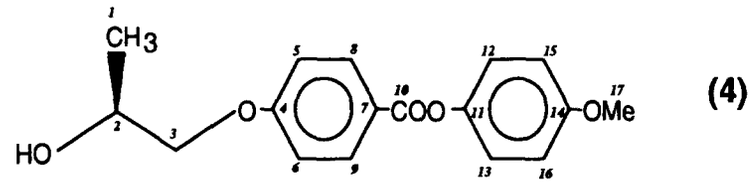

Carbon number	Chemical shift δ	Carbon number	Chemical shift δ
1	18.8	12, 13	122.3
17	55.4	8, 9	132.0
2	65.9	11	144.3
3	73.3	14	157.0
5, 6	114.2	4	162.7
15, 16	114.3	10	165.0
7	122.1		

continued for 50 min, by which time the solution was a pale green colour, then a solution of the tosylate (25 g, 90 mmol) in DMF (35 ml) was added slowly dropwise. After the addition, the temperature was raised to 70°C and stirring continued for 15 h. DMF was removed from the reaction mixture by co-evaporation with xylene *in vacuo*; then chloroform (250 ml) and water (250 ml) were added. The separated organic layer was washed three times with a 20 wt% potassium hydroxide solution (3 × 200 ml) followed by water (2 × 200 ml), then dried over magnesium sulfate. The concentrated mixture was finally subjected to flash chromatography using chloroform as the eluant, giving **3** as a straw-coloured oil (pure by thin layer chromatography (TLC)). Yield 27.4 g (81%). $[\alpha]_D = -10.86°$. $C_{22}H_{26}O_6$ (386 g mol^{-1}): C 68.40%, H 6.73% (calculated); C 68.12%, H 7.05% (found).

Compound 4. The tetrahydropyranyl-protected compound (**3**) (27 g, 70 mmol) was deprotected by dissolving it in acidified ethanol (1 vol% solution of 0.1 M HCl in 350 ml of ethanol); the mixture was then refluxed for 25 min, by which time TLC analysis indicated that only the product alcohol was present. Ethanol was evaporated *in vacuo* then chloroform (250 ml) and water (250 ml) were added. The organic layer was separated and washed with two further portions of water, then dried over magnesium sulfate. The solvent was removed and the residue was recrystallized (chloroform and a small amount of hexane) to afford the product as fine white crystals. Yield 20.52 g (94%); m.p. 102–103°C; $[\alpha]_D = +12.00°$.

^1H n.m.r. ($CDCl_3$). $\delta = 1.35$ (d; 3H) methine C-CH_3, 3.85 (s; 3H) ArOCH_3, 3.85–4.1 (m; 2H) -CH_2OAr, 4.25 (m; 1H) methine H, 6.9–8.2 (m; 8H) ArH.

Table 2 ^{13}C n.m.r. peak chemical shift values for compound **1**

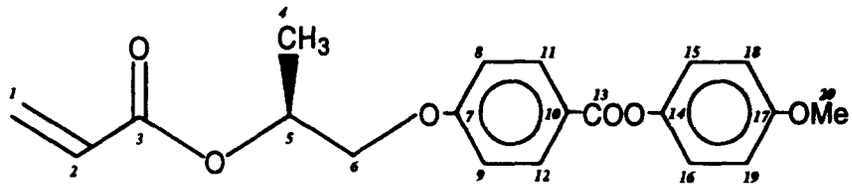

Carbon number	Chemical shift δ	Carbon number	Chemical shift δ
4	16.5	2	128.3
20	55.4	1	131.0
5	68.5	11, 12	132.1
6	70	14	144.4
8, 9	114.3	17	157.1
18, 19	114.3	7	162.6
10	112.2	13	165
15, 16	112.4	3	165.4

Table 3 Details of the copolymerization of monomer **1** with monomer **2** in benzene at 60°C

Copolymer	f_1[a]	Time (h)	Conversion (%)	F_1[a]	M_n (g mol^{-1})[b]	M_w/M_n
2	0.00	24.0	60	0.00	35 500	1.93
3a	0.05	4.0	10	0.05	41 600	2.11
3b	0.10	4.0	12	0.13	27 200	2.42
3c	0.15	3.5	9	0.16	47 400	1.95
3d	0.25	4.5	13	0.28	31 500	2.46
3e	0.30	6.5	10	0.35	53 400	2.00
3f	0.50	4.5	7	0.50	31 600	2.38
3g	0.75	4.0	12	0.77	32 100	1.92
1	1.00	48.0	62	1.00	54 700	2.23

[a] See text for an explanation of f_1 and F_1
[b] M_n in polystyrene equivalents, determined by gel permeation chromatography measurements. The solvent used for precipitation purposes was chloroform. The precipitant (non-solvent) in all cases was cold methanol

^{13}C n.m.r. ($CDCl_3$). The peak chemical shift values for the ^{13}C-decoupled spectrum of compound **4** are shown in *Table 1*. Chemical shifts for CH_3 CH_2 and CH groups were determined from the DEPT spectrum. $C_{17}H_{18}O_5$ (302 g mol^{-1}): C 67.54%, H 5.96% (calculated); C 67.60%, H 6.20% (found).

Monomer 1. Acryloyl chloride (5.1 g, 56 mmol) was added slowly dropwise to an ice-cooled, stirred solution of the chiral alcohol **4** (19.83 g. 56 mmol), triethylamine (5.86 g, 58 mol) and 2,6-di-t-butyl-4-methylphenol (~0.5 g) in anhydrous chloroform (250 ml). After the addition, the ice bath was removed and the solution stirred vigorously overnight. The reaction mixture was then diluted with chloroform (200 ml) and the mixture washed with water (2 × 200 ml), 10 wt% sodium hydroxide solution (2 × 200 ml) and finally water (100 ml). After drying the organic layer over magnesium sulfate, the solvent was removed and the residue purified by flash chromatography using chloroform as the eluant. The pure monomer **1** was obtained as a white powdery solid. Yield 20.81 g (89%); m.p. 68–70°C. $[\alpha]_D = 35.2°$.

^1H n.m.r. ($CDCl_3$). $\delta = 1.35$ (d; 3H) methine C-CH_3, 3.85 (s; 3H) ArOCH_3, 4.15 (dd; 2H) -CH_2OAr, 5.30 (sextuplet; 1H) methine H, 5.8–6.5 (m; 3H) vinylic H, 6.9–8.2 (m; 8H) ArH.

^{13}C n.m.r. ($CDCl_3$). The peak chemical shift values for the compound are shown in *Table 2*.

4-Cyanophenyl-4'-(6-acryloyloxyhexyloxy) benzoate (2). Monomer **2** was prepared as reported elsewhere[7].

Copolymerizations

Homo- and copolymerization reactions were carried out in benzene at 60°C using a 0.5 mol% of recrystallized 2,2'-azobisisobutyronitrile as an initiator. Monomers were dissolved in the solvent and oxygen was removed by repeated freeze–thaw cycles before sealing the reaction ampoules under vacuum. For the copolymers, conversions were kept below 15% to minimize composition drift, and materials were recovered by precipitation into a non-solvent such as methanol or diethyl ether. Samples were purified by dissolution–reprecipitation, then dried under vacuum for 24 h at 60°C. Copolymer compositions were estimated using ^1H n.m.r. by comparison of the integrated values of two separate distinguishable resonances corresponding to a distinct environment in each of the comonomers.

Characterization

Monomers and polymers were characterized by ^1H

n.m.r. and ^{13}C n.m.r. using a Bruker 200 MHz instrument and by elemental analysis.

Thermal analysis was effected using a Perkin–Elmer DSC-2 differential scanning calorimeter and glass transition temperatures, T_g, were taken at the extrapolated onset of the baseline shift.

Molar masses were determined, in polystyrene equivalents, using a Waters 590 GPC. Characterization details for the copolymer samples are given in *Table 3*.

Optical characterization. Liquid crystalline phases and textures were identified using an Olympus BH2 polarizing microscope fitted with a Linkham PR600 hot stage accessory, and the viewing platform was a video camera and monitor.

The wavelength of selective reflection λ_R for the chiral nematic copolymer samples was determined in two ways:

(i) Absorption measurements were effected using a Shimadzu u.v./vis. spectrophotometer with specially designed heated cells (a sample and a reference), comprising two quartz plates between which the polymer samples were sandwiched to create a thin film. Heating elements attached to both were controlled by a Duratrak V6HM transformer with a K-type thermocouple attached to a Digitron 3900 thermometer, as the temperature monitor. Absorption spectra were recorded first in the isotropic phase then at a constant reduced temperature $T^* = (T/T_i)$, where T is the measuring temperature and T_i the clearing temperature[3], then quenched rapidly below room temperature to 'lock in' the liquid crystalline structure in the polymer glass. The value of λ_R was then obtained from the difference between the spectrum of the sample in the isotropic phase and that of the sample in the liquid crystalline phase. Annealing of the samples in the liquid crystalline state was found to improve the definition of the spectral peak as the alignment of the liquid crystal phase with respect to the cell walls was improved. Good alignment of the liquid crystal phase in the observation cell is essential if narrow reflectance bands are to be obtained in the spectra. Our normal practice is to use clean glass or quartz plates, that have been rubbed in one direction several times with a tissue, as the cell walls, but this is not wholly effective and alternative methods are now being examined.

(ii) Specular reflectivity measurements were carried out on a Perkin–Elmer Lambda 9 u.v./vis. near-i.r. spectrophotometer. Samples were placed on a quartz disc and heated into the isotropic melt, after which a second disc was placed on top and sheared to give a thin film. The sample was cooled to the appropriate T^* where it was annealed for up to 24 h. Wavelengths of the reflected light could then be measured for each sample as a function of copolymer composition.

RESULTS AND DISCUSSION

Copolymerization

The copolymer composition F_1, expressed as the mole fraction of **1** in the copolymer, is shown in *Figure 1*,

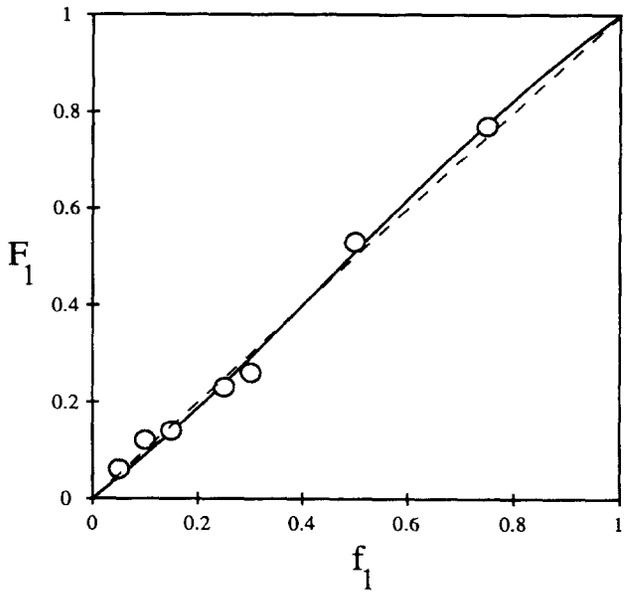

Figure 1 Plot of copolymer feed composition f_1 against the copolymer composition F_1 expressed in mole fractions of monomer **1**. The dotted line represents an ideal copolymerization; the solid line is a computer fit of the experimental data

Table 4 The glass transition and phase transition temperatures of polymers and copolymers (g, glassy; N*, chiral nematic; i, isotropic)

Copolymer	f_1	T_g (°C)	T_{N^*-i} d.s.c. (°C)[a]	T_{N^*-i} HSM (°C)[b]	Remarks
2	0.00	28	140[c]	140[c]	Marbled nematic homopolymer
3a	0.05	31	128	128[d]	Nematic texture
3b	0.10	33	122	124[d]	Nematic texture
3c	0.15	35	119	119[d]	Nematic texture
3d	0.25	37	112	115	Chiral nematic planar texture
3e	0.30	39	108	111	Chiral nematic planar texture
3f	0.50	47	102	102	Chiral nematic planar texture
3g	0.75	59	92	94	Strong birefringence upon shearing
1[e]	1.00	67	–	78	Weak birefringence upon shearing

[a] T_{N^*-i} d.s.c. (°C) refers to the temperature of transition from the liquid crystal to the isotropic phase recorded by d.s.c. during the second heating scan at 20°C min^{-1} (recorded as the temperature of maximum heat flow)
[b] T_{N^*-i} HSM (°C) refers to the temperature at which birefringence disappears totally; recorded using hot stage microscopy
[c] This temperature corresponds to the nematic to isotropic transition in the case of the homopolymer **2**
[d] Chiral copolymers which appear to have nematic textures observed using HSM
[e] No liquid crystal phase detected using d.s.c.

plotted as a function of the feed composition f_1 (the mole fraction of **1** in the feed).

The data were fitted using a non-linear least squares program based on the terminal model, and it can be seen that the copolymerization reaction is close to ideal behaviour. The reactivity ratios estimated from this method are $r_1 = 1.26 \pm 0.08$ and $r_2 = 1.18 \pm 0.06$. Consequently, larger samples of these copolymers could be prepared for further study by allowing the reactions to run to higher conversions without much drift in composition occurring.

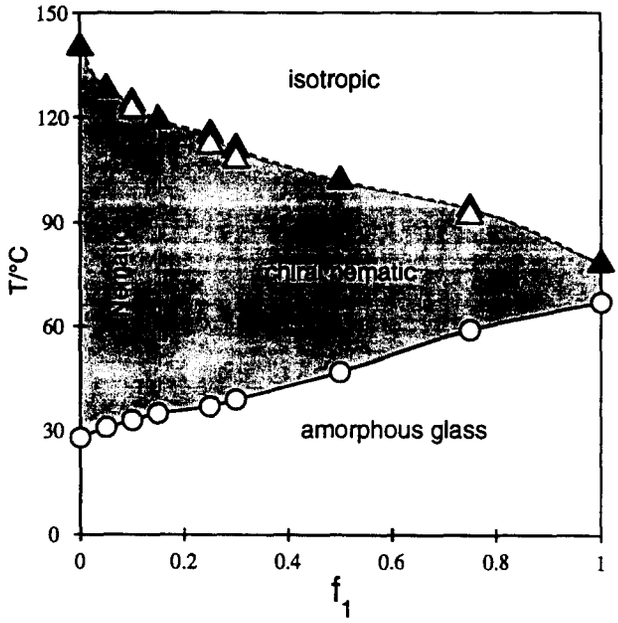

Figure 2 Dependence of T_g (O), T_{N^*-i} (recorded by hot stage microscopy) (▲) and T_{N^*-i} (recorded by d.s.c.) (△) on the copolymer feed composition

While the values of M_n quoted in *Table 1* are in polystyrene equivalents, the molar masses of the samples can be regarded as being high enough to assume that the mesophase transition temperatures are independent of the sample chain length[1].

Thermal and optical properties

Details of the T_g values and the liquid crystalline phase transition temperatures for each of the samples are summarized in *Table 4*.

The homopolymer of **2** exhibited the classical marbled texture of a nematic liquid crystal phase when heated above the T_g, and the phase passed into the isotropic liquid state at 140°C. However, no liquid crystal phase could be detected for the homopolymer of **1** when examined using d.s.c., although a weak birefringence could be observed on the hot stage microscope when the sample was sheared. This effect disappeared on heating the sample above 78°C, suggesting that a weak liquid crystal phase, stable only over an 11°C range, was present.

Copolymerization of **1** and **2** produced a series of samples (**3a**–**3g**) in which the T_g increased as the amount of unit **1** in the copolymer increased. This was accompanied by a concomitant decrease in the clearing temperature T_{N^*-I} and a narrowing of the range of temperature over which the liquid crystal phase was stable.

These trends are best expressed graphically, as in *Figure 2*, which shows more clearly the rapid restriction of the liquid crystal phase as the content of the chiral monomer **1** in the copolymer becomes greater.

Copolymers **3a**–**3c**, with low concentrations of **1** in their chains, exhibit weak first-order endothermic liquid crystal to isotropic transitions in the d.s.c. heating curves. Supercooling of the samples was slight as the ($i = N^*$) transition was detected only 4°C lower than the clearing temperature on the heating cycle. None of these samples exhibited chiral nematic phases, as cooling from the isotropic melt produced only a pale, fine sanded

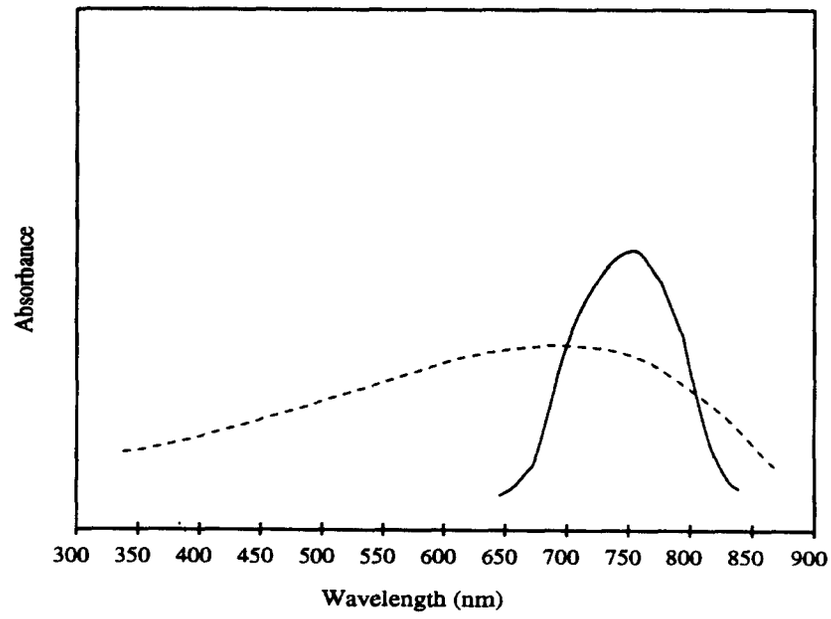

Figure 3 Absorbance spectrum for sample **3d**. The broken line is for the unannealed sample, while the solid line is the spectrum after annealing for 24 h

texture for **3a** which coarsened on cooling, and marbled textures for **3b** and **3c** after annealing the samples for some time. These were all considered to indicate the presence of nematic phases only. A further increase in the content of **1** ($F_1 \geq 0.28$) led to changes in the optical texture of samples **3d**–**3g**, all of which exhibited only one mesophase. Sample **3d** had a pale blue homogeneous planar texture formed on cooling from the isotropic melt. Further cooling led to a slow change in the reflection colour through the visible spectrum, to an orange-red colour. Similar behaviour was observed on cooling **3e** and **3f**, except that each had its own specific temperature-dependent range of colours. These reflected colours passed through the reverse order of colour change on reheating the samples. Reference to equation (1) indicates that as the peak wavelength of selective

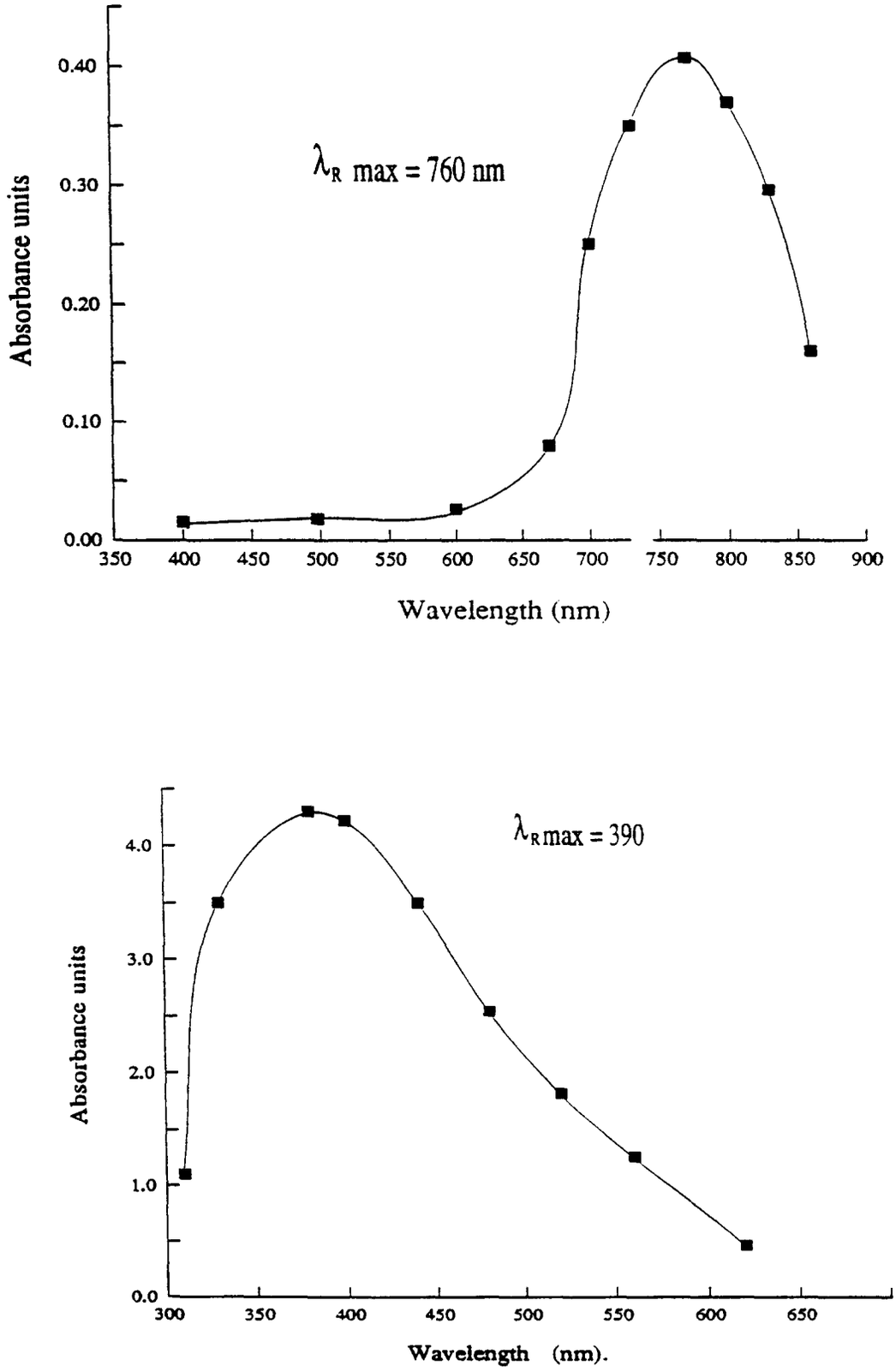

Figure 4 Absorbance spectrum for sample **3e** (upper diagram) and **3f** (lower diagram)

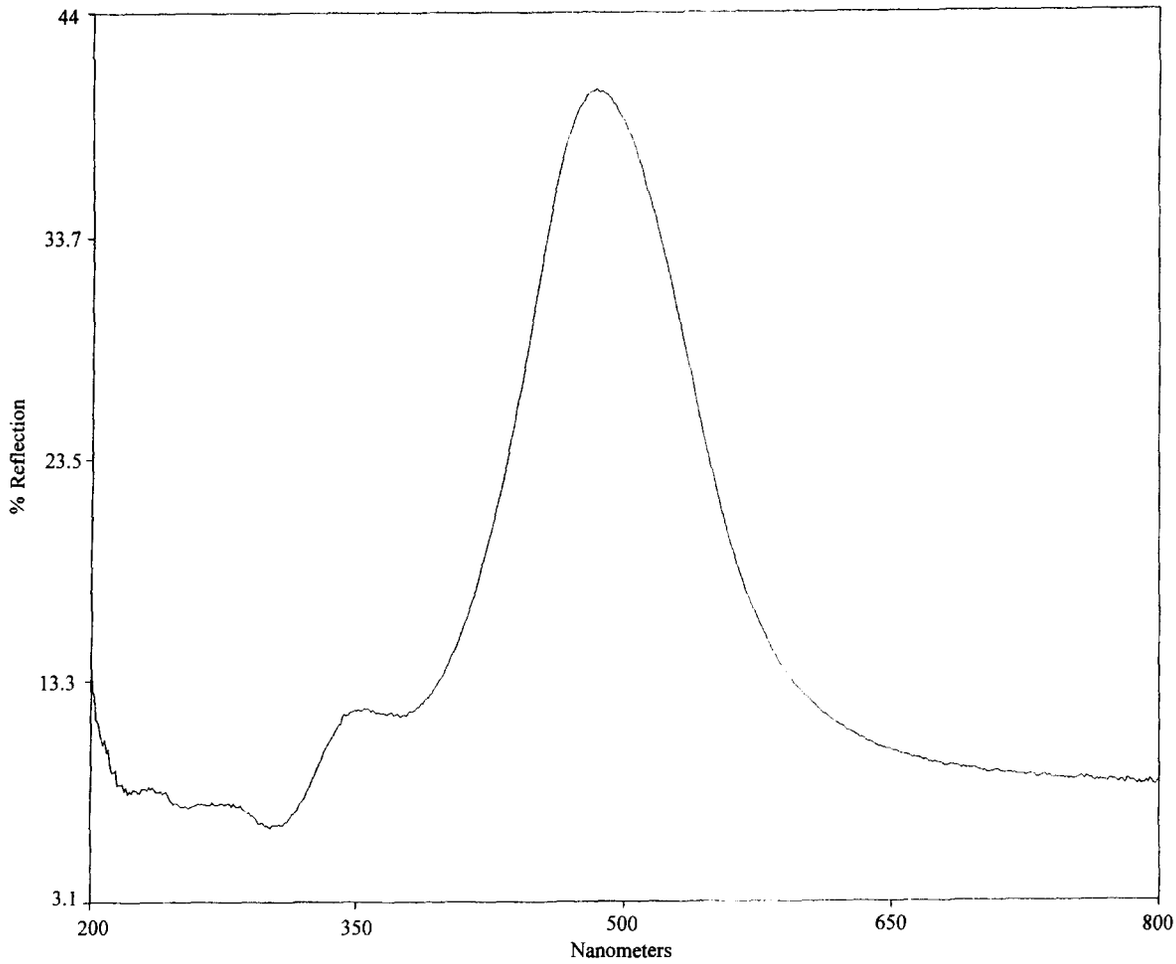

Figure 5 Percentage reflectivity as a function of wavelength from specular reflection measurements for a sample with composition $F_1 = 0.4$ prepared and measured by Mr J. Thies

reflection is proportional to the helical pitch, then there is an unwinding of the helical structure with a decrease in temperature towards T_g and the glassy state. As there is no smectic phase intervening between the chiral nematic state and T_g, the copolymers can be quenched rapidly in the liquid crystal phase, thereby locking that structure into the glass[1]. Consequently, stable films can be prepared that reflect the λ_R pertaining to the temperature from which the sample was quench cooled. This procedure can be used to prepare samples for comparison of their λ_R under defined conditions.

A fixed reduced temperature $T^* \sim 0.88$ was selected at which to anneal samples **3d**–**3f**, after which they were quenched into the glassy state. The λ_R for each was measured as described, and the absorption spectra are shown in *Figures 3* and *4*. As illustrated in *Figure 3*, annealing was found to sharpen the reflection spectrum, probably due to an improvement in the alignment of the helical structures with respect to the quartz plates of the measuring cells. The reflection spectra of additional samples of this copolymer series, prepared by Thies, were measured and included in *Figure 6* to supplement the data. The spectrum of a sample with $F_1 = 0.4$ is presented in *Figure 5*, and indicates that the amount of reflection was about 40%. For a perfectly aligned sample, the maximum value would be 50%[1].

A function called the helical twisting power (HTP) can be used to estimate the effect of copolymer composition on the pitch of the helical structures found in the chiral

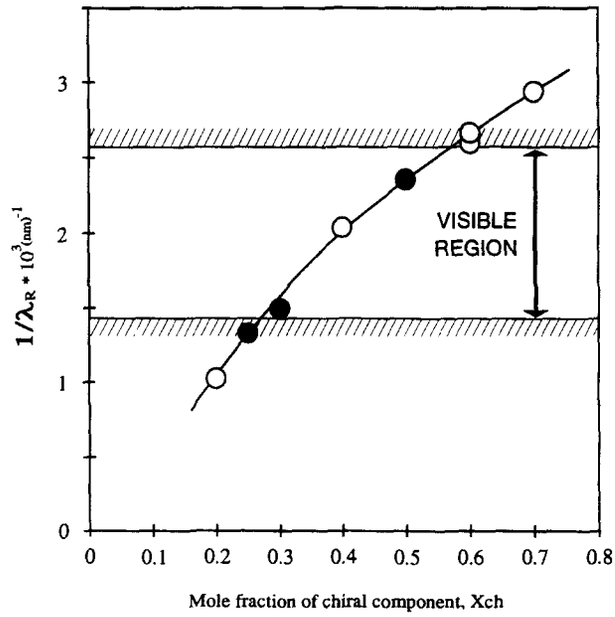

Figure 6 Dependence of the inverse selective reflection wavelength $(\lambda_R)^{-1}$ on the mole fraction of the chiral monomer **1** in the copolymers. ●, λ_R measured by differential absorption spectrometry; ○, λ_R obtained from specular reflection, measured by J. Thies

nematic phase. This was originally defined[8], for mixtures of small chiral guest molecules in a nematic host, as the slope of P^{-1} plotted as a function of the mole fraction of the chiral molecules in the mixture X_{ch}, i.e.

$$HTP = \frac{dP^{-1}}{dX_{CH}} = \tilde{n}\frac{d(\lambda_R)^{-1}}{dX_{CH}} \quad (2)$$

This can be used here by replacing X_{CH} with F_1, the mole fraction of the chiral units in the copolymer, as shown in *Figure 6*. The data are best represented by a curve, but the initial portion, from $F_1 = 0$ up to $F_1 \sim 0.4$ is approximately linear and $(HTP/\tilde{n})$ can be estimated to be 5×10^{-3} nm^{-1}. This is of similar magnitude to values for cholesteryl esters in a nematic polymer host[1], but much lower than copolymers containing non-chiral mesogens and cholesteryl side-groups[3,4]. Clearly the twisting power of **1** is much weaker than cholesterol derivatives. Finkelmann and Rehage[1,9] also reported values for siloxane copolymers in which the chiral monomer was prepared using *S*-(−)-2-methyl-1-butanol, which has a much lower specific optical rotation than cholesterol, as the terminal unit.

The *HTP* was less pronounced in this series (*viz.* 2.04×10^{-3} nm^{-1}) than in both the cholesterol derivatives and the copolymers reported here. This parameter obviously depends on a number of factors. For example, Finkelmann and Rehage showed that the *HTP* decreased as the length of the spacer units in the comb-branch polymers increased[3], similarly the nature of the chiral centre and, as will be demonstrated in a later publication[10], the position of the chiral centre relative to the mesogen can also have an effect on the structure of the helix formed in the chiral nematic phase.

CONCLUSIONS

It has been demonstrated in the copolymer series reported here, comprising chiral and non-chiral mesogens, that samples in a restricted composition range exhibit the optical properties associated with a chiral nematic structure. Because of the absence of a smectic phase, this structure can be retained in the glassy state on quench cooling from the nematic phase and so these systems offer the possibility of preparing coatings that can selectively reflect up to 50% of a specific wavelength of light. Measurements of λ_R by absorption and specular reflection gave self-consistent results and the effectiveness of the chiral centre in inducing a helical twist in the N* phase could be estimated from these data. An understanding of the structural factors governing these effects should then allow the more facile preparation of materials with particular optical properties, and this forms part of an ongoing study in this laboratory.

ACKNOWLEDGEMENTS

The authors are grateful to EPSRC for a studentship award (TH) and for additional financial support from Courtaulds Coatings. They also thank Mr J. Thies for specular reflection measurements on samples from an extended copolymer series.

REFERENCES

1 Finklemann, H. and Rehage, G. *Adv. Polym. Sci.* 1984, **60/61**, 99
2 De Vries, H. *Acta Crystallogr.* 1950, **4**, 219
3 Finkelmann, H. and Rehage, G. *Makromol. Chem. Rapid Commun.* 1980, **1**, 783
4 Finkelmann, H. and Rehage, G. *Makromol. Chem. Rapid Commun.* 1982, **3**, 859
5 Cowie, J. M. G. and Hunter, H. W. *Makromol. Chem.* 1991, **191**, 1393
6 Cowie, J. M. G. and Hunter, H. W. *Makromol. Chem.* 1991, **192**, 143
7 Cowie, J. M. G. and Hunter, H. W. *J. Polym. Sci., Polym. Chem., Part A* 1993, **31**, 1179
8 Finkelmann, H. and Stegemeyer, H. *Ber. Bunsenges. Phys. Chem.* 1978, **82**, 1302
9 Finkelmann, H. *Philos. Trans. R. Soc. London, Ser. A* 1983, **309**, 105
10 Cowie, J. M. G. and Hinchcliffe, T. (unpublished)